Jpn. J. Appl. Phys. Vol. 42 (2003) pp. 4249–4252
Part 1, No. 7A, July 2003

Low Dark Current InGaAs(P)/InP p–i–n Photodiodes

Yen-Wei CHEN, Wei-Chou HSU*, Rong-Tay HSU[1], Yue-Huei WU[1] and Yeong-Jia CHEN

Institute of Microelectronics, Department of Electrical Engineering, National Cheng-Kung University, 1 University Road, Tainan, Taiwan 70101, R.O.C.
[1]*South Epitaxy Corporation, No. 16 Da-Shun 9th Road, Tainan Science-Based Industrial Park, Hsin-Shi, Tainan County, Taiwan 744, R.O.C.*

(Received October 18, 2002; accepted for publication February 18, 2003)

Planar InGaAs(P)/InP p–i–n photodiodes have been successfully fabricated by low-pressure metalorganic chemical vapor deposition (LP-MOCVD). High-quality and uniform epitaxial layers are obtained. It is noted that the InGaAs layer background concentration is as low as $4.5 \times 10^{13}\,cm^{-3}$. The dark current is significantly reduced by using a wider-band-gap material of quaternary $In_xGa_{1-x}As_yP_{1-y}$ as a cap layer to reduce the device surface leakage current. In addition, the device becomes highly photosensitive due to the reduction of the absorption of the radiation in the narrow-band-gap $In_xGa_{1-x}As_yP_{1-y}$ cap layer. The p–i–n photodiode with a wide-band-gap InP cap layer exhibits a dark current as low as 60 pA at -10 V bias, corresponding to a dark current density of $4.2 \times 10^{-7}\,A/cm^2$. [DOI: 10.1143/JJAP.42.4249]

KEYWORDS: LP-MOCVD, PIN photodiode, $In_xGa_{1-x}As_yP_{1-y}$

1. Introduction

A long-wavelength optical transmission system operating at 1.0 to 1.65 μm wavelength region has attracted considerable attention due to its low-loss and low-dispersion optical characteristics. As one of the key components, semiconductor photodetectors based on InP materials, which offer the advantages of low dark current, high-efficiency and high-speed operation, have been widely studied for long-wavelength optical fiber communication applications.[1–7] Therefore, although p–i–n photodetectors do not have internal gain, a combination of a photodetector with an amplification device, such as high electron mobility transistor (HEMT) or heterojunction bipolar transistor (HBT), in optoelectronic integrated circuits (OEIC's) has led high-sensitivity optical receivers to operate for high-rate data transmission.[8–12] In order to achieve these characteristics, it requires a precise control of the thickness and concentration of different epitaxial layers. Moreover, a reduction of InGaAs absorption layer background concentration for reducing the device dark current can bring significant improvement in receiver sensitivity. Therefore, it is necessary to produce pure epitaxial layers as well as those that have few defects.[13]

Mixed quaternary $In_xGa_{1-x}As_yP_{1-y}$ alloys with various band-gaps (cover the energy-gap from 1.35 eV (InP) to 0.75 eV ($In_{0.53}Ga_{0.47}As$), and the corresponding wavelength range from 0.92 to 1.65 μm at 300 K) can be grown on InP substrates with perfect lattice matching for detecting various wavelength regions. Unfortunately, the resulting difficult fabrication technology of a quaternary $In_xGa_{1-x}As_yP_{1-y}$ alloy, which contains both group V elements of As and P in the epitaxial layer simultaneously rather than a ternary $In_xGa_{1-x}As$, is obtained.[14–17] For $In_xGa_{1-x}As$ material growth, lattice composition is determined solely by the ratio of TMIn/TMGa, independent of growth temperature, growth rate and V/III ratio. However, for quaternary $In_xGa_{1-x}As_yP_{1-y}$ material growth, the relative incorporation of As and P atoms strongly depends on various growth parameters. Furthermore, uniform composition is also a problem for epitaxial techniques.

In this paper, we propose planar InGaAs(P)/InP photodiodes with various band-gaps of quaternary InGaAsP cap layers grown by low-pressure metalorganic chemical vapor desposition (LP-MOCVD). The planar p–i–n photodiodes exhibit high-quality and uniform epitaxial layers. It is noted that the InGaAs layer background concentration is as low as $4.5 \times 10^{13}\,cm^{-3}$. In addition, the quaternary $In_xGa_{1-x}As_yP_{1-y}$ alloys with various band-gaps are well lattice matched to InP with uniform composition. The p–i–n photodiode with a wider-band-gap quaternary $In_xGa_{1-x}As_yP_{1-y}$ alloy cap layer is applied to reduce the device surface leakage current and thus to improve device dark current characteristics. The p–i–n photodiode with a wide-band-gap InP cap layer exhibits a dark current as low as 60 pA at -10 V bias (device diameter is 135 μm), corresponding to a dark current density of $4.2 \times 10^{-7}\,A/cm^2$.

2. Device Fabrication

The studied structures were grown by an LP-MOCVD system on S-doped N^+-InP substrates. The detail epitaxial layers of the studied planar InGaAs(P)/InP p–i–n photodiodes are shown in Table I. The deposition temperature was 640°C and the reactor pressure was held at 100 mbar. Trimethylindium (TMIn), trimethylgallium (TMGa), arsine (AsH_3) and phosphine (PH_3) were used as the In, Ga, As and P sources, respectively. Disilane (Si_2H_6) was adopted as the n-type source. The uniformity in layer thickness of InP and InGaAs(P) under the above-mentioned growth conditions is ±5%. The lattice mismatch of InGaA(P) is kept within ±500 ppm, measured by X-ray diffraction. A summary of the quaternary $In_xGa_{1-x}As_yP_{1-y}$ material characteristics is shown in Table II. The quaternary $In_xGa_{1-x}As_yP_{1-y}$ materials with various compositions, which correspond to various band-gaps and wavelengths, are well controlled in the proposed structures. A schematic cross section of the studied planar InGaAs(P)/InP p–i–n photodiodes is shown in Fig. 1.

Table I. Details of epitaxial layers of the studied planar InGaAs(P)/InP p–i–n photodiodes.

Structure	Thickness	A1	A2	A3	B1	B2	B3
Cap layer	1 μm	InP	1.1 PQ	1.4 PQ	InP	1.05 PQ	1.1 PQ
Absorption layer	2.5 μm	InGaAs	InGaAs	InGaAs	1.4 PQ	1.4 PQ	1.4 PQ
Buffer layer	0.5 μm	InP	InP	InP	InP	InP	InP
Substrate	350 μm	InP	InP	InP	InP	InP	InP

*Corresponding author. E-mail address: wchsu@eembox.ncku.edu.tw

Table II. A summary of the quaternary $In_xGa_{1-x}As_yP_{1-y}$ material characteristics.

Material	Composition	Wavelength (μm)	Energy-gap
InP	InP	0.92	1.35
1.05 PQ	$In_{0.89}Ga_{0.11}As_{0.24}P_{0.76}$	1.05	1.18
1.1 PQ	$In_{0.85}Ga_{0.15}As_{0.33}P_{0.67}$	1.1	1.13
1.4 PQ	$In_{0.66}Ga_{0.34}As_{0.73}P_{0.27}$	1.4	0.89
InGaAs	$In_{0.53}Ga_{0.47}As$	1.65	0.75

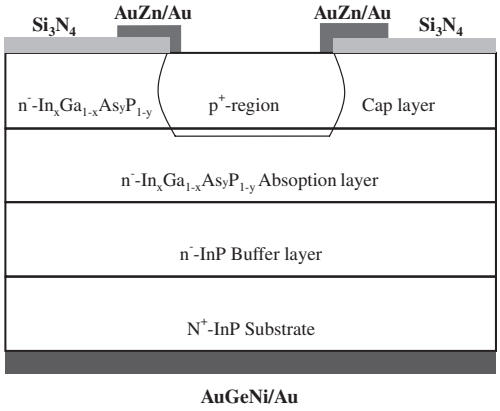

Fig. 1. Schematic cross section of the studied planar InGaAs(P)/InP p–i–n photodiodes.

2500 Å dielectric layer Si_3N_4 was deposited by plasma-enhanced chemical vapor deposition (PECVD) as a diffusion mask with local openings. A planar photodiode can provide high reliability due to the surface that is passivated during device fabrication. The p^+–n junction was formed in the InGaAs(P) absorption layer by diffusing Zn through the InGaAs(P) cap layer. AuGeNi/Au and AuZn/Au were adopted as the n- and p-type ohmic contact metals, respectively.

3. Experimental Results

For a reversely biased p–i–n photodiode device, it is important to minimize the device dark current and obtain high-speed response. The carrier transit time can be shortened by reducing the thickness of the absorption layer, reducing the device dark current and obtaining a high-speed response. However, reducing the absorption layer thickness usually leads to a lower quantum efficiency. Minimizing absorption layer background concentration in the depletion region is the most desirable method of increasing device performance. The intrinsic-like material ensures a higher possible mobility, thus improving carrier transit time and device operation speed. In an MOCVD process, the major growth parameters for obtaining high-quality materials include growth temperature, V/III ratio, deposition rate, source molecules, carrier gas and other considerations. Some of our studies have shown that high growth temperature (630–660°C) and low V/III ratio (particularly for the $In_{0.53}Ga_{0.47}As$ material, the V/III ratio is as low as 10) are necessary for the growth of high-purity InGaAs(P) materials. Therefore, under the above-mentioned growth conditions, high-quality and low-background-concentration InGaAs(P) materials are achieved. Figures 2(a) and 2(b) show the

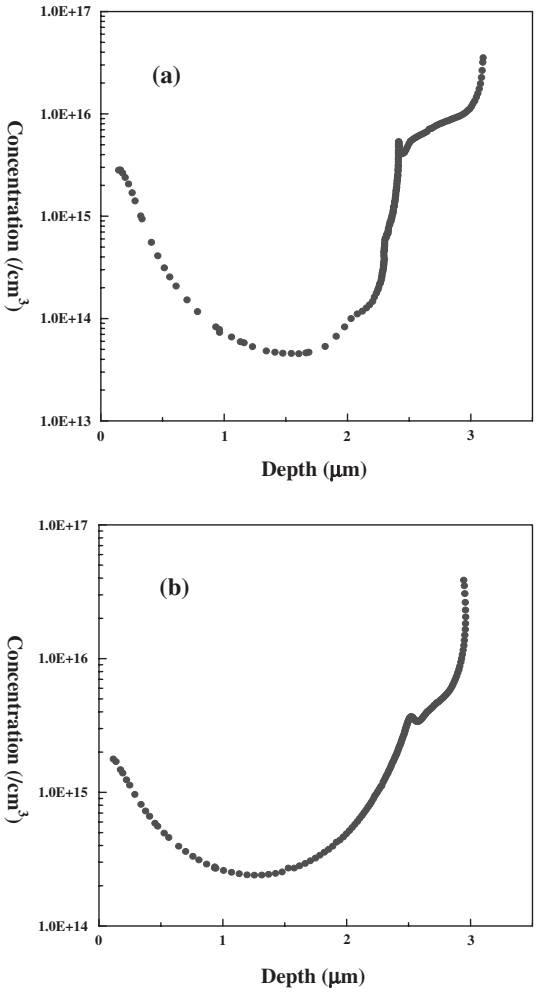

Fig. 2. Doping concentrations of (a) $In_{0.53}Ga_{0.47}As$ and (b) $In_{0.66}Ga_{0.34}As_{0.73}P_{0.27}$ layers of the studied InGaAs(P)/InP p–i–n photodiodes measured based on the *C–V* profile.

doping concentrations of $In_{0.53}Ga_{0.47}As$ and $In_{0.66}Ga_{0.34}As_{0.73}P_{0.27}$ (1.4 PQ) layers of the studied InGaAs(P)/InP p–i–n photodiodes measured based on the *C–V* profile. The measured concentrations of $In_{0.53}Ga_{0.47}As$ and $In_{0.66}Ga_{0.34}As_{0.73}P_{0.27}$ absorption layers are as low as 4.5×10^{13} and $2.4 \times 10^{14}\,cm^{-3}$, respectively. We believe that device performances can be significantly improved due to the excellent material quality.

Figure 3 shows the dark current characteristics of the studied $In_xGa_{1-x}As_yP_{1-y}/In_{0.53}Ga_{0.47}As/InP$ photodiode with an InP cap layer (structure A1) at various temperatures. The measured dark current at 300 K is as low as 60 pA ($4.2 \times 10^{-7}\,A/cm^2$) at −10 V bias. The low dark current is attributed to the excellent material quality. In general, for low fields, the dark current consists of generation–recombination current and diffusion current. We observe that the dark current increases with increasing temperature. This is due to the fact that increasing temperature enhances the generation recombination current and the diffusion current, thus increasing the device dark current.

Figure 4 shows the reverse current-voltage characteristics of the studied $In_xGa_{1-x}As_yP_{1-y}/In_{0.53}Ga_{0.47}As/InP$ photodiodes with different-band-gap InGaAsP cap layers. The wavelengths of $In_xGa_{1-x}As_yP_{1-y}$ cap layers of various compositions are 0.92, 1.1 and 1.4 μm. The dark currents

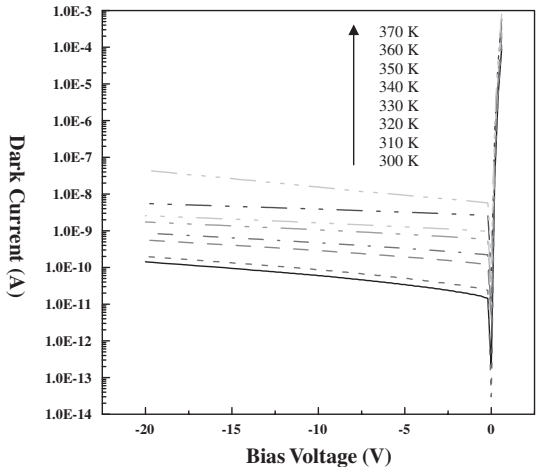

Fig. 3. Dark current characteristics of the studied InP/$In_{0.53}Ga_{0.47}As$/InP photodiode at various temperatures.

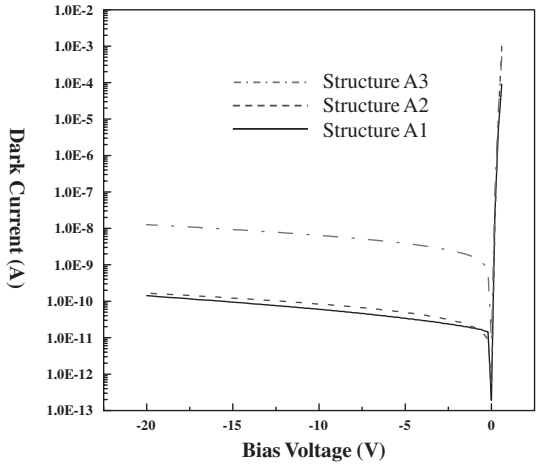

Fig. 4. Dark current–voltage characteristics of the studied $In_xGa_{1-x}As_yP_{1-y}$/$In_{0.53}Ga_{0.47}As$/InP photodiodes with different InGaAsP cap layers.

of structures A1, A2 and A3 measured at −10 V are 60 pA, 84 pA and 6.4 nA, respectively. The results show that the dark currents of structures A1 and A2 with higher-band-gap cap layers are much lower than that of structure A3 with a lower-band-gap cap layer. We believe that the further reduction of dark current in structures A1 and A2 is related to the differences in surface effect and interface properties between dielectric and InGaAsP. The generation-recombination current and the diffusion current can be expressed as[14)]

$$I_{g\text{–}r} \propto \exp(-E_g/2kT), \quad (1)$$

$$I_{diff} \propto \exp(-E_g/kT), \quad (2)$$

where E_g is the energy-gap and kT is the Boltzman energy.

From eqs. (1) and (2), we assume that generation-recombination current and diffusion current generated by the InGaAs absorption layer of the studied structures A1, A2 and A3 are almost the same. For a higher-band-gap $In_xGa_{1-x}As_yP_{1-y}$ cap layer structure, the generation–recombination current and the diffusion current generated by the $In_xGa_{1-x}As_yP_{1-y}$ cap layer may be reduced due to the higher-energy-gap material. Furthermore, for the studied $In_xGa_{1-x}As_yP_{1-y}$/InGaAs/InP structure, the valence band discontinuity (ΔE_V) at the $In_xGa_{1-x}As_yP_{1-y}$/InGaAs heterointerface also increases with the higher band-gap of the $In_xGa_{1-x}As_yP_{1-y}$ material. The valence band discontinuities (ΔE_V) of InP/$In_{0.53}Ga_{0.47}As$, $In_{0.85}Ga_{0.15}As_{0.33}P_{0.67}$ (1.1 PQ)/$In_{0.53}Ga_{0.47}As$ and $In_{0.66}Ga_{0.34}As_{0.73}P_{0.27}$ (1.4 PQ)/$In_{0.53}Ga_{0.47}As$ heterojunctions are about 0.35, 0.23 and 0.08 eV, respectively. For a higher-band-gap cap layer structure (A1 or A2) under a reverse bias, it is difficult for the holes in the $In_{0.53}Ga_{0.47}As$ absorption layer to have sufficient energy to surmount the barrier height and transfer to the $In_xGa_{1-x}As_yP_{1-y}$ cap layer due to the high potential barrier between $In_xGa_{1-x}As_yP_{1-y}$/$In_{0.53}Ga_{0.47}As$ heterojunctions, thus reducing the device reverse leakage current. Therefore, the dark current characteristics of the studied $In_xGa_{1-x}As_yP_{1-y}$/InGaAs/InP structure can be further reduced by using a higher-band-gap $In_xGa_{1-x}As_yP_{1-y}$ material as the cap layer. Consequently, the lowest dark current is expected in structure A1 with an InP cap layer, which has the widest band-gap among $In_xGa_{1-x}As_yP_{1-y}$ material systems, compared to structures A2 and A3.

Figure 5(a) shows the dark current–voltage characteristics of the studied $In_xGa_{1-x}As_yP_{1-y}$/1.4 PQ/InP photodiodes with

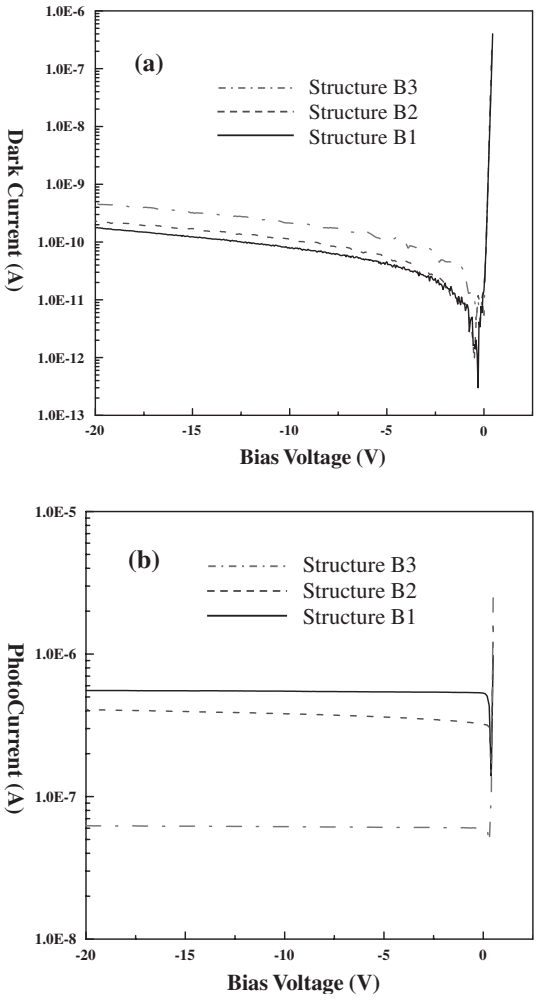

Fig. 5. (a) Dark current–voltage characteristics of the studied $In_xGa_{1-x}As_yP_{1-y}$/1.4 PQ/InP photodiodes with different InGaAsP cap layers. (b) Photocurrent–voltage characteristics of the studied $In_xGa_{1-x}As_yP_{1-y}$/1.4 PQ/InP photodiodes with different InGaAsP cap layers.

different InGaAsP cap layers. The wavelengths of $In_xGa_{1-x}As_yP_{1-y}$ cap layers of various compositions are 0.92, 1.05 and 1.1 μm. The dark currents of structures B1, B2 and B3 measured at −10 V are 78 pA, 110 pA and 213 pA, respectively. The results also show that the lower dark current characteristics can be obtained in the structure with a higher-band-gap cap layer material due to the lower generation–recombination current and diffusion current generated by the higher bandgap cap layer. Figure 5(b) shows photocurrent–voltage characteristics (under a microscope) of the studied structures B1, B2 and B3. The photocurrents of structures B1, B2 and B3 measured at −10 V are 549 nA, 381 nA and 61 nA, respectively. The results show that higher photocurrent, which corresponds to higher responsivity, can be obtained in the structure with a higher-band-gap cap layer. The cap layer material requires careful attention since the incident light must traverse it and finally be absorbed in the absorption layer. Therefore, using a narrower-band-gap InGaAsP material as the cap layer may cause more incident light absorption in the cap layer, because of the reduction of the incident light traversing the cap layer into absorption lower photocurrent in the structure. In addition, at 1.3 μm, a dc responsivity of 0.81 A/W was measured at −5 V bias in structure B1 with an InP cap layer, which is higher than those of structures B2 and B3. The p-i-n photodiode with a wide-band-gap InP cap layer in the $In_xGa_{1-x}As_yP_{1-y}$ material system can be expected to further improve device performances.

4. Conclusions

We have successfully fabricated and demonstrated a series of planar $In_xGa_{1-x}As_yP_{1-y}$ p–i–n photodiodes grown by MOCVD. The background concentration of the high-quality InGaAs absorption layer is as low as $4.5 \times 10^{-13}\,cm^{-3}$. Using a wide-band-gap InP material as the cap layer, the device surface leakage current and the dark current are significantly reduced. In addition, the wide-band-gap cap layer may also reduce the incident light absorption in the cap layer, thus improving device responsivity.

Acknowledgement

Authors would like to acknowledge the support of all members of the South Epitaxy Corporation involved in this project. This work was also supported by the National Science Council of the Republic of China under contract No. NSC90-2215-E-006-014.

1) S. Miura, H. Kuwatsuka, T. Mikawa and O. Wada: J. Lightwave Technol. **5** (1987) 1371.
2) K. S. Park, D. K. Oh, H. M. Kim and K. E. Pyun: IEE Electron Lett. **34** (1998) 79.
3) N. Emeis, M. Schier, L. Hoffmann, H. Heinecke and B. Baur: IEE Electron Lett. **28** (1992) 344.
4) N. Susa, H. Nakagome, O. Mikami, H. Ando and H. Kanbe: IEEE J. Quantum Electron. **16** (1980) 864.
5) T. P. Lee, C. A. Burrus and A. G. Dentai: IEEE J. Quantum Electron. **17** (1981) 232.
6) C. L. Ho, M. C. Wu, W. J. Ho, J. W. Liaw and H. L. Wang: IEEE J. Quantum Electron. **36** (2000) 333.
7) S. R. Forrest, I. Camlibel, O. K. Kim, H. J. Stocker and J. R. Zuber: IEEE Electron Device Lett. **2** (1981) 283.
8) P. Berthier, L. Giraudet, A. Scavennec, D. Rigaud, M. Valenza, J. I. Davies and S. W. Bland: J. Lightwave Technol. **12** (1994) 2131.
9) N. Shimizu, K. Murata, A. Hirano, Y. Miyamoto, H. Kitabayashi, Y. Umeda, T. Akeyoshi, T. Furuta and N. Watanbe: IEE Electron Lett. **36** (2000) 1220.
10) Y. Muramoto, K. Kato, Y. Akahori, M. Ikeda, A. Kozen and Y. Itaya: IEEE Photon. Technol. Lett. **7** (1995) 685.
11) M. J. Kim, D. K. Kim, S. J. Kim and M. B. Das: IEEE Trans. Electron Devices **44** (1997) 551.
12) M. Yung, J. Jensen, R. Walden, M. Rodwell, G. Raghavan, K. Elliott and W. Stanchina: IEEE J. Solid-State Circ. **34** (1999) 219.
13) M. Gallant, N. Puetz, A. Zemel and F. R. Shepherd: Appl. Phys. Lett. **52** (1988) 733.
14) O. K. Kim, B. V. Dutt, R. J. Mccoy and J. R. Zuber: IEEE J. Quantum Electron. **21** (1985) 138.
15) I. Kim, D. G. Chang and P. D. Dapkus: J. Cryst. Growth **195** (1996) 138.
16) S. R. Forrest: IEEE J. Quantum Electron. **17** (1981) 217.
17) M. B. Yi, J. Paslaski, Y. Y. Liu, T. R. Chen and A. Yariv: IEE Electron Lett. **24** (1988) 455.